Libyan Journal of Science & Technology 7:2 (2018) 127–132

Faculty of Science - University of Benghazi

Libyan Journal of Science & Technology

(Formerly known as Journal of Science & It's Applications)

journal home page: www.sc.uob.edu.ly/pages/page/77

Effect of sintering temperature on the electrical properties of a nanocomposite electrolyte based on calcium-doped ceria/ternary carbonate

Ibrahim A. Amar [a,b,*], Mohammed M. Ahwidi[a], Mohammed Zidan[a], Ihssin Abdalsamed[a], Asmaa Ali[a]

[a]*Department of Chemistry, Faculty of Science, Sebha University, Sebha Libya*

[b]*Central Laboratory at Sebha University, Sebha Libya*

ARTICLE INFO

Article history:
Received 01 May 2018
Revised 26 July 2018
Accepted 30 August 2018
Available online 03 September 2018

Keywords:
Ionic conductivity, ceria/carbonate composite electrolyte, composite effect, impedance spectroscopy

* Corresponding author:
E-mail address: ibr.amar@sebhau.edu.ly
I. A. Amar

ABSTRACT

In this study, the effect of sintering temperature on the proton-and oxygen-ion conductivities of a nanocomposite electrolyte based on Ca-doped ceria/carbonate was investigated. Ca-doped ceria (CDC) nanoparticles were successfully synthesised using a sol-gel process. Ternary carbonate eutectic salt ($(Li/Na/K)_2CO_3$) was prepared by solid-state reaction. A dual-phase nanocomposite was prepared by mixing CDC with the ternary carbonate at a weight ratio of 70:30. The prepared materials were characterised by X-ray diffraction (XRD) and thermal analysis (TGA-DSC). The fabricated green nanocomposite pellets were sintered at two different temperatures (600 and 700°C). AC Impedance spectroscopy was used to measure the ionic conductivities of the composite electrolyte within the range of temperature from 300 to 600°C. The proton ion (H^+) conductivities at 600°C were found to be 0.33 and 0.37 S cm^{-1} for samples sintered at 600 and 700°C, respectively. The oxygen ion (O^{2-}) conductivities at 600°C for samples sintered at 600 and 700°C were found to be 0.35 and 0.27 S cm^{-1}, respectively. The nanocomposite electrolyte was thermally stable in both atmospheres (oxidising and reducing). The results suggest that the nanocomposite can be used as an electrolyte material for the electrochemical devices operating within low to intermediate temperature range.

© 2018 University of Benghazi. All rights reserved.

1. Introduction

Doped-ceria based oxides represent an important class of promising materials for the application as electrolytes for intermediate to low-temperature solid oxide fuel cells (IT/LT-SOFCs) (Chourashiya *et al.*, 2008; Singh *et al.*, 2007; Steele, 2000). Among these oxides, samarium and gadolinium-doped ceria ($Ce_{0.8}Sm_{0.2}O_{2\delta}$ and $Ce_{0.8}Gd_{0.2}O_{2-\delta}$) exhibit the highest ionic conductivity (Inaba and Tagawa, 1996; Mogensen *et al.*, 2000; Steele, 2000). In addition, co-doping strategy has also been employed to further improve the ionic conductivity of singly-doped ceria-based electrolytes such as Sm-doped ceria (SDC) or Gd-doped ceria (GDC). In this regard, several studies have been carried out with the aim of investigating the effect of co-doping on the electrical properties of ceria-based electrolytes (Guan *et al.*, 2008; Wang *et al.*, 2004). However, these dopants (Sm and Gd) are very expensive. In terms of material's cost, calcium ion (Ca^{2+}) is a cheap and readily available, thus, it can be used in place of these costly dopants (Banerjee *et al.*, 2007). Despite the fact that the electrical properties of ceria were improved using single- and co-doping strategies, these approaches could not eliminate the electronic conduction in pure ceria which is resulted from the reduction of Ce^{4+} to Ce^{3+} at high temperature in H_2-containing atmosphere (Raza *et al.*, 2010). The issue related to Ce^{4+} reduction can be overcome by mixing doped ceria (e.g., SDC or GDC) with various salts (e.g., halides, sulphates, hydrates, carbonates) (Liu *et al.*, 2010).

Among ceria/salt electrolytes, ceria-carbonate composites (3C) have drawn considerable attention as promising electrolyte materials for the application in low to intermediate operating temperature electrochemical devices (Wang *et al.*, 2012). These composite materials are two-phase electrolytes, the first phase (host phase) is doped ceria (e.g., SDC or GDC) and the second phase is alkali carbonate (e.g., Na_2CO_3, $(Li/Na)_2CO_3$, $(Li/Na/K)_2CO_3$) (Ali *et al.*, 2018; Raza *et al.*, 2012; Wang *et al.*, 2012; Zhu *et al.*, 2013). The addition of carbonate phase not only results in the ionic conductivity enhancement but also suppresses the Ce^{4+} reduction in H_2-containing atmosphere and at high temperature (Fan *et al.*, 2017; Wang *et al.*, 2012). Compared to pure doped ceria (e.g., SDC), doped ceria composite electrolytes have the following advantages; high ionic conductivity (>0.1 S cm^{-1}) above 300°C, fast ionic transport, ternary ionic ($O^{2-}/H^+/CO_3^{2-}$) conduction, negligible electronic conduction and thermal stability in both oxidising and reducing atmospheres (Amar *et al.*, 2017a; Fan *et al.*, 2017; Raza *et al.*, 2012; Wang *et al.*, 2012; Xia *et al.*, 2009).

Because of their aforementioned properties, doped-ceria-carbonate composites have been used as electrolyte materials in different applications including; solid oxide fuel cells (SOFCs) (Khan *et al.*, 2017; Raza *et al.*, 2010), ammonia synthesis (Amar *et al.*, 2014; Amar *et al.*, 2011), direct carbon fuel cells (DCFCs) (Li *et al.*, 2009; Liu *et al.*, 2008), water electrolysis (Zhu *et al.*, 2006) and carbon dioxide (CO_2) permeation membrane (Li *et al.* 2009). The recent advances in doped-ceria carbonate composite electrolytes and their possible applications have been reviewed, recently (Fan *et al.*, 2017; Fan *et al.*, 2013; Wang *et al.*, 2012; Zhu *et al.*, 2013).

Based on the results of earlier studies, it was found out that the ionic conductivities of ceria-carbonate composite based electrolytes are affected by several factors including; ceria phase (i.e., undoped, singly-doped or co-doped), alkali carbonate phase (i.e., single, binary or ternary), method of preparation, carbonate content and pellet sintering temperature, etc. (Ali *et al.*, 2018; Amar *et al.*, 2018; Fan *et al.*, 2017; Khan *et al.*, 2017; Liu *et al.*, 2010; Ristoiu *et al.*, 2012).

In a previous work, Ca-doped ceria (CDC) was synthesised via co-precipitation (Amar *et al.*, 2017a). It was then mixed with ternary carbonate (CDC-$(Li/Na/K)_2CO_3$, 80:20 wt%) and sintered in air at 600°C. At 600°C, the oxygen-ion (O^2) and proton-ion (H^+) conductivities of the composite were about 0.12 and 0.13 S cm^{-1}, respectively. In the present study, Ca-doped ceria was successfully

synthesised by sol-gel process. The effect of pellet sintering temperature on the oxygen-ion (O^{2-}) and proton-ion (H^+) conductivities of Ca-doped ceria/ternary carbonate (70:30 wt%) are investigated. In addition, the ionic conductivities of the ceria-carbonate composite electrolyte were investigated using AC impedance spectroscopy (IS) from 300 to 600°C.

2. Experimental

2.1 Chemicals

Calcium nitrate tetrahydrate ($Ca(NO_3)_2{\cdot}4H_2O$, 99 %), cerium nitrate hexahydrate ($Ce(NO_3)_3{\cdot}6H_2O$, 99 %), lithium carbonate (Li_2CO_3, 98 %), citric acid ($C_6H_8O_7$, 99 %), ethylenediaminetetraacetic acid, EDTA, ($C_{10}H_{18}N_2O_8$, 99 %) and potassium carbonate (K_2CO_3, 99 %) were purchased from Alfa Aesar. Sodium carbonate (Na_2CO_3, 99.5 %) was purchased from Sigma Aldrich. Nitric Acid (HNO_3, 70 %) and ammonia solution (35 %) were purchased from Fisher.

2.2 Synthesis of materials

$Ce_{0.8}Ca_{0.2}O_{2-\delta}$ (CDC) powder was synthesised via a sol-gel method using citric acid and EDTA as complexing agents (Gao *et al.* 2009). In brief, stoichiometric amounts of $Ce(NO_3)_3{\cdot}6H_2O$ and $Ca(NO_3)_2{\cdot}4H_2O$ were dissolved in a minimum amount of deionised water. Citric acid and EDTA were added to the metal cations solution in a molar ratio of 1.5:1:1. A dilute ammonia solution was then added to adjust the pH of the mixed solution to around 6. A hotplate was used for stirring and evaporating the mixed solution to dryness. The formed solid product was collected and ground before being calcined in air at 700°C for 2 h to form the desired material (CDC). Fig. 1 shows a flowchart for the overall sol-gel experiment used for CDC powder synthesis. The ternary carbonate eutectic salt $(Li/Na/K)_2CO_3$ and CDC-$(Li/Na/K)_2CO_3$ composite electrolyte were prepared by solid-state reaction. Briefly, the ternary carbonate eutectic salt that composed of Li_2CO_3, Na_2CO_3, K_2CO_3 in a molar ratio of 43.5:31.5:25 was calcined in air at 600°C for 1 h. The CDC-$(Li/Na/K)_2CO_3$ composite was obtained after the heat treatment of the CDC and $(Li/Na/K)_2CO_3$ mixture (70:30 wt%) in the air at 600°C for 1 h. The detailed information for preparing the ternary carbonate and the CDC-carbonate composite is described elsewhere (Amar *et al.*, 2014).

2.3 Characterisation

TGA-DSC analysis of the CDC dried gel (ash) and the nanocomposite (CDC-carbonate) was carried out using a Stanton Redcroft STA/TGH thermal analyser (STA 1500 series). The CDC dried gel was heated in air at constant heating/cooling rate of 10°C min^{-1} from room temperature up to 800°C. The CDC-$(Li/Na/K)_2CO_3$) samples were heat treated in O_2 and 5% H_2-Ar atmospheres from room temperature to 600°C with a heating/cooling rate of 10°C min^{-1}. The XRD patterns were recorded at room temperature using a Panalytical X'Pert Pro diffractometer with Cu$K\alpha$ radiation (λ= 1.5405 Å). From the XRD peaks, the average crystallite sizes (D) and the lattice parameters (a) of the materials under investigation were estimated using the following Eqs. (Fu *et al.*, 2010).

$$D = \frac{0.9\,\lambda}{(\beta\cos\theta)} \tag{1}$$

$$d_{hkl} = \frac{\lambda}{2sin\theta} \quad ; \quad a = d_{hkl}\sqrt{h^2+k^2+l^2} \tag{2}$$

where β is the full width at half maximum (FWHM) of the peak in radiance, λ is the wavelength of the X-ray, θ is the Bragg angle, d is the interplanar distance and khl are the Miller indices.

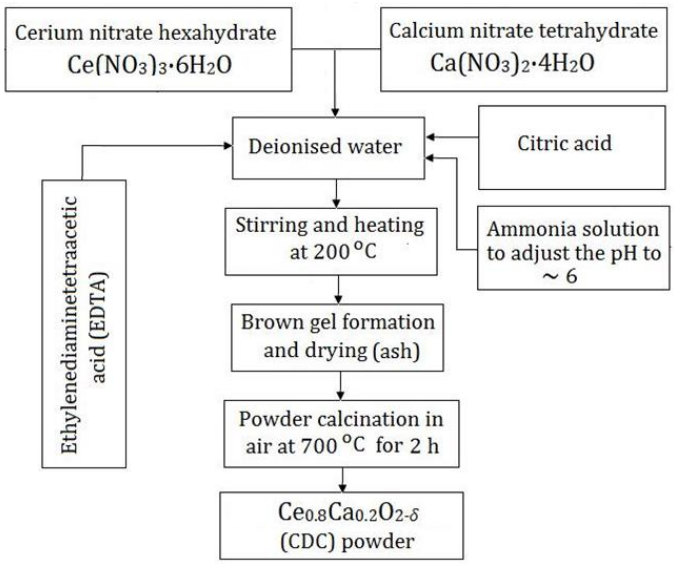

Fig. 1 A schematic representation of sol-gel process used for $Ce_{0.8}Ca_{0.2}O_{2-\delta}$ (CDC) powder synthesis.

2.4 Pellets preparation for conductivity measurements

The CDC-$(Li/K/Na)_2CO_3$ powder was cold-pressed at a pressure of 259 MPa into circular pellets with 13 mm diameter and~ 2 mm thickness. After pressing, the green pellets were sintered in air for 2 h at 600 and 700°C with a constant heating/cooling rate of 2°C. Then, both sides of the sintered pellets were coated with a silver paste before being fired in the air at 550°C for 30 min to form Ag electrodes with a porous structure. A schematic representation of pellets preparation is shown in Fig. 2

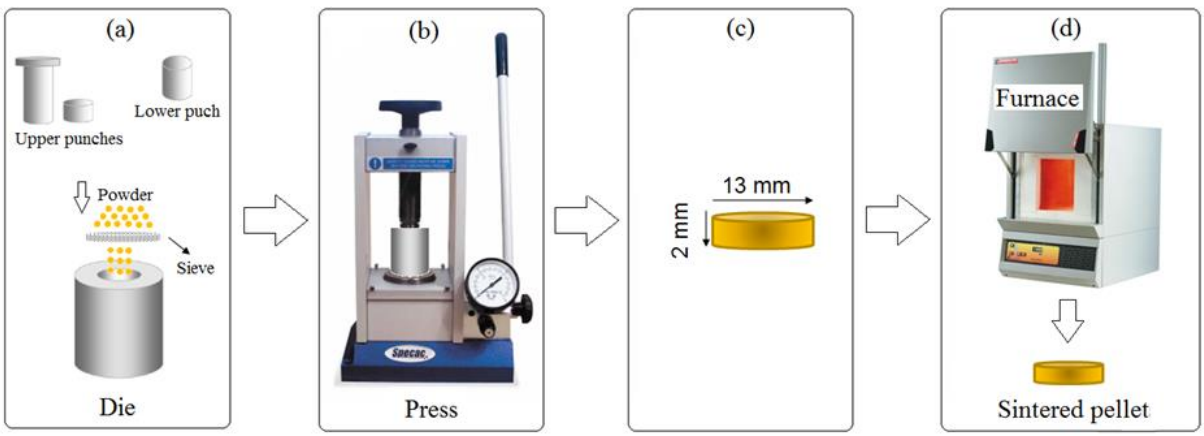

Fig. 2 Schematic representation of pellets preparation; (a) die filling; (b) powder pressing; (c) green pellet; (c) pellet sintering.

Impedance spectroscopy (IS) technique was used to investigate the AC ionic conductivity using a Solartron Analytical instrument (1470E) with AC amplitude of 100 mV, over the range of frequency from 1 MHz up to 0.01 Hz and 10 points per decades. The measurements were carried out using a pseudo 4-probe configuration in the presence of either dry O_2 or wet 5% H_2-Ar from 300 to 600°C. Eq. 3 (Jaiswal *et al.*, 2015) and Eq. 4 (Fu *et al.*, 2010) were used to estimate the AC ionic conductivities and the activation energies of the proposed electrolyte, respectively.

$$\sigma = \frac{L}{RA} \tag{3}$$

$$\sigma T = \sigma_0 exp\left(-\frac{E_a}{kT}\right) \tag{4}$$

where σ is the conductivity (S cm^{-1}), L is the sample thickness (cm), R is the resistance (Ω), A is the cross-sectional area of the specimen (cm^2), T is the absolute temperature, σ_0 the pre-exponential factor, E_a is the activation energy (eV) and k is Boltzmann constant.

3. Results and discussion

3.1 Thermal analysis characterisation

The thermal decomposition of the CDC gel precursor (ash) in air from room temperature up to 800°C is shown in Fig. 3. The TGA-DSC graph shows different weight loss processes accompanied by endothermic or exothermic events. Upon heating (from 25 to 250°C), a small endothermic peak, which could be due to the loss of the residual water in gel precursor, was observed at 120°C (Zarkov *et al.*, 2016). At the temperature of 250 to 500°C, a strong exothermic peak was observed at 334°C. This event could be due to the pyrolysis of the metal nitrates and organic compounds (citric acid and EDTA) complexes (Patra *et al.*, 2011). In addition, from 700 to 800°C, no obvious weight change was noticed, as shown in the TGA curve (Fig. 3). Thus, the as-prepared CDC powder was calcined at 700°C.

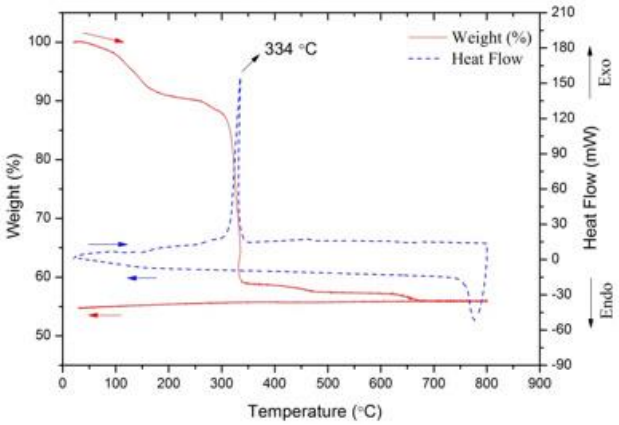

Fig. 3 TGA-DSC curves of the as-prepared CDC powder.

Figs. 4a & b show the TGA-DSC curves of CDC-(Li/K/Na)$_2$CO$_3$ nanocomposite from room temperature to 600°C in O_2 and 5% H_2-Ar, respectively. Upon heating, two endothermic events accompanied with weight losses were observed in both tested atmospheres (O_2 and 5% H_2-Ar). The first peak was located at 104 and 106°C for samples tested in O_2 (Fig. 4a) and 5% H_2-Ar (Fig.4b), respectively. This peak could be ascribed to the loss of adsorbed water. The second peak was observed at 385 °C and 383 °C for samples studied in O_2 and 5% H_2-Ar, respectively. This event can be due to the ternary carbonate ((Li/K/Na)$_2$CO$_3$) melting point (~400 °C) (Janz and Lorenz, 1961). Upon cooling, one exothermic peak was observed at 356 and 345°C for samples tested in O_2 and 5% H_2-Ar, respectively. This event can be ascribed to recrystallization of the ternary carbonate (Amar *et al.*, 2017b). In addition, the total weight loss in the composite electrolyte under the heat treatment was about 2% in O_2 and 3% in 5% H_2-Ar. This means that the composite electrolyte (CDC-(Li/K/Na)$_2$CO$_3$) is thermally stable in the oxidising and reducing atmospheres within the measured temperature range.

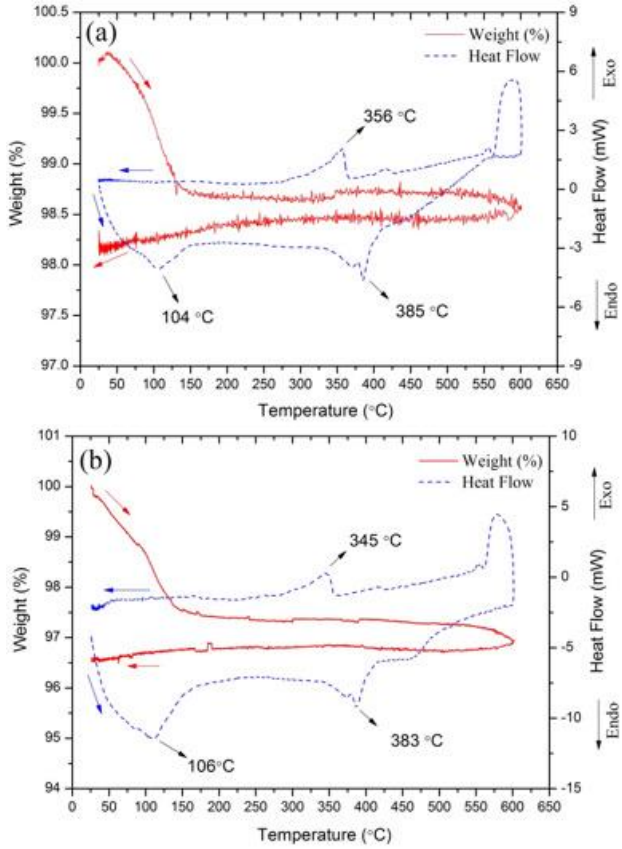

Fig. 4 TGA-DSC curves of CDC-carbonate composite electrolyte; (a) in O_2; (b) 5% H_2-Ar.

3.2 XRD analysis

The X-ray diffraction patterns of pure CDC and CDC-carbonate composite electrolyte are shown in Figs. 5a & b, respectively. A single phase of CDC was obtained after firing its corresponding gel precursor at 700 °C in air for 2 h (Fig. 5a). In addition, the all detected peaks in XRD patterns of CDC and CDC-carbonate are indexed to a cubic fluorite structure of CeO_2 (JCPDS 34-0394). Apart from CDC phase, no additional peaks were observed in the case of CDC-carbonate composite electrolyte (Fig. 5b). This means that the ternary carbonate exists in the composite electrolyte as an amorphous phase (Ali *et al.*, 2018; Khan *et al.*, 2017). The average crystallite size of pure CDC was found to be 10.52 nm and that of CDC-(Li/Na/K)$_2$CO$_3$ was about 19.33 nm. The lattice parameters (a=b=c) were 5.4219 Å and 5.4135 Å for CDC and CDC-(Li/Na/K)$_2$CO$_3$, respectively. These lattice parameters values are similar to that reported for CDC (5.4157 Å) (Tanwar *et al.*, 2018), and slightly larger than that reported for CeO_2 (5.4019 Å) (Kim, 1989). This increase in the lattice parameters is resulted from the partial substitution of Ce^{4+} by Ca^{2+} that has a large ionic size (1.12 Å) compared to Ce^{4+} (0.97 Å) (Cho *et al.*, 2008; Shannon and Prewitt, 1969). In addition, the volumes of the unit cells (a^3) of CDC and CDC-(Li/Na/K)$_2$CO$_3$ were about 159.389 (Å)^3 and 158.65 (Å)^3, respectively.

3.3 Electrical conductivity

AC impedance spectroscopy (IS) technique was used to measure the CDC-carbonate ionic conductivities. Fig. 6a & b show the typical impedance spectroscopy plots in dry O_2 and wet 5% H_2-Ar atmospheres at 300 and 600°C, respectively. Under dry O_2, two semicircles were observed in both cases (300 and 600°C). At high frequency, small incomplete semicircle was resolved at each temperature. This semicircle is corresponding to the electrolyte contribution. At low frequency, a large depressed semicircle related to

the electrode process was resolved when the impedance was recorded at 300 and 600°C. Under wet 5% H_2-Ar, only large depressed semicircle related to electrode process and long tail corresponding to electrode/electrolyte interface were resolved at low frequency when the impedance was recorded at 600 and 300°C, respectively (Di *et al.*, 2010; Jaiswal *et al.*, 2015). The electrolyte contribution was not observed due to the short time constant of bulk and grain response (Di *et al.*, 2010).

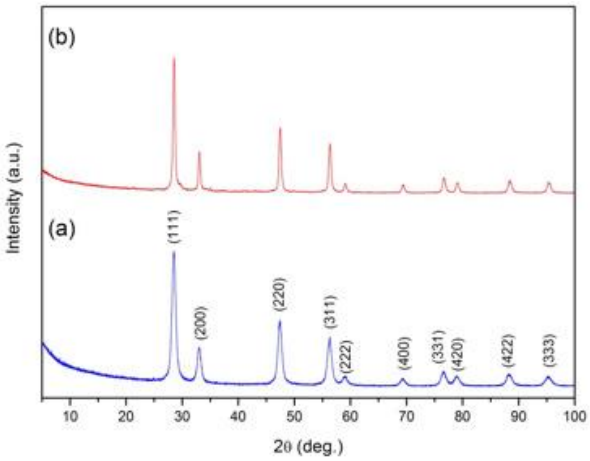

Fig. 5 X-ray diffraction patterns of; (a) CDC calcined at 700°C for 2 h, (c) CDC-ternary carbonate calcined at 600°C for 1 h.

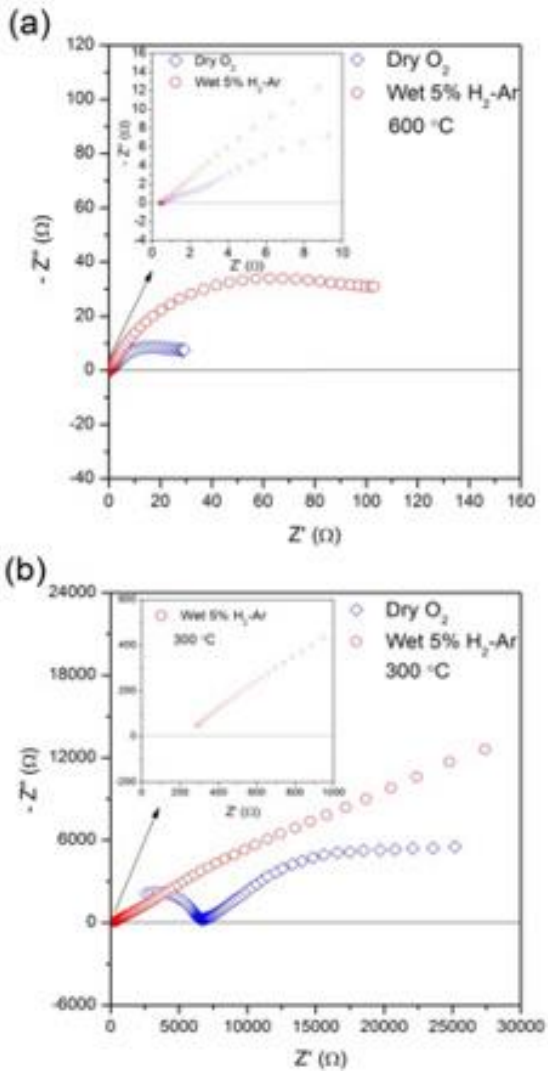

Fig. 6 AC impedance spectra of CDC-carbonate nanocomposite in dry O_2 and wet 5% H_2-Ar. (a) at 600 °C; (b) at 300°C.

The total ionic conductivities of the CDC-carbonate nanocomposite was measured in the presence of either dry O_2 and wet 5% H_2-Ar within the operating temperature range of 300 to 600°C. The green pellets of CDC-carbonate were sintered at two different temperatures (600 and 700°C) with the aim of studying the effect of sintering temperature on their ionic conductivities. It is clearly seen that the electrical conductivities follow the similar trend in both tested atmospheres. It can be noticed from Figs. 7a and b that, the ionic conductivities for samples sintered at 600 and 700°C increased significantly by increasing the measuring temperature from 300 to 600°C. It can be also seen that there was a jump in the ionic conductivities above the carbonate melting point. This enhancement in the ionic conductivities could be due to the composite effect which will provide a fast conduction pathway for all mobile ions (i.e. O^{2-}, H^+, Na^+, K^+, Li^+, HCO_3^- and CO_3^{2-}) at interfacial region between the two phases (ceria and carbonate) (Li *et al.*, 2007).

Under O_2 and H_2-containing atmospheres, the overall measured ionic conductivities are attributed to the oxygen-ion (O^{2-}) and proton-ion (H^+) conductivities, respectively. In the case of dry O_2, at 600 °C, the O^{2-}-ion conductivity of pellet sintered at 600°C (0.35 S cm^{-1}) was slightly higher than that sintered at 700 °C (0.27 S cm^{-1}), as presented in Fig. 7a. These values are higher than that of Ca-doped ceria (~10^{-3} S cm^{-1}) at 600 °C (Ma *et al.*, 2012). However, below 500°C, the sample sintered at 700°C exhibits the highest ionic conductivity (Fig. 7a). In doped-ceria/carbonate composite electrolytes, the O^{2-} ions are transported via the ceria phase and interfacial region between the two phases (Khan *et al.*, 2013; Wang *et al.*, 2011).

Under H_2-containing atmosphere, the H^+-ion conductivity of the sample sintered at 700°C was higher than that sintered at 600°C (Fig. 7b). This can be due to the fact that, at the high sintering temperature, a better contact was formed at the interface between Ca-doped ceria and the ternary carbonate which in turn resulted in a high ionic conduction pathway (Xia *et al.*, 2011). Recently, Muhammed *et al.*, (2015) have examined the effect of the sample sintering temperature on the surface morphology and the electrical properties of SDC-$(Li/Na)_2CO_3$) composite. In that study, the observed ionic conductivity enhancement was due to the fact that the right sintering temperature resulted in getting better surface morphology, carbonate distribution, interfacial microstructure, etc. At 600°C, the H^+-ion conductivity was about 0.33 S cm^{-1} for sample sintered at 600°C and 0.37 S cm^{-1} for sample sintered at 700°C. These values of ionic conductivities are higher than that reported for GDC-$(Li/Na/K)_2CO_3$ (0.29 S cm^{-1}) and lower than that reported for CGDC-$(Li/Na/K)_2CO_3$ (0.52 S cm^{-1}) (Amar *et al.*, 2014; Amar *et al.*, 2017b). In contrast to oxygen-ion conduction, the proton-ion conduction in doped-ceria/carbonate composite occurs only at interfacial region between ceria and the carbonate phase (Khan *et al.*, 2013; Wang *et al.*, 2011).

In general, the ionic conductivities (O^{2-} and H^+) of the CDC-carbonate composite electrolyte were higher than those of CDC-$(Li/Na/K)_2CO_3$ (80:20 wt%), as reported in a previous work (Amar *et al.*, 2017a). This variation in the ionic conductivities can be due to the difference the carbonate contents and sample sintering temperatures. Fig. 8 shows a comparison between the oxygen-ion and proton-ion conductivities for the sample sintered at 700°C. It is clearly seen that the proton-ion conductivities of the CDC-carbonate composite were higher than oxygen-ion conductivities. This indicates that CDC-carbonate composite electrolyte is mainly proton-ion conductor at this operating condition.

The activation energies (E_a) of the CDC-carbonate nanocomposite in two atmospheres (dry O_2 and wet 5% H_2-Ar) were calculated from Arrhenius plots (insets of Figs. 7a & b) within the temperature range of 450–600°C. In the case of dry O_2, the activation energies were about 0.55±0.22 eV and 0.43±0.05 eV for pellets sintered at 600 and 700°C, respectively. In wet 5% H_2-Ar, the activation energies were about 0.60±0.17 eV and 0.44±0.06 eV for pellets sintered at 600 and 700°C, respectively.

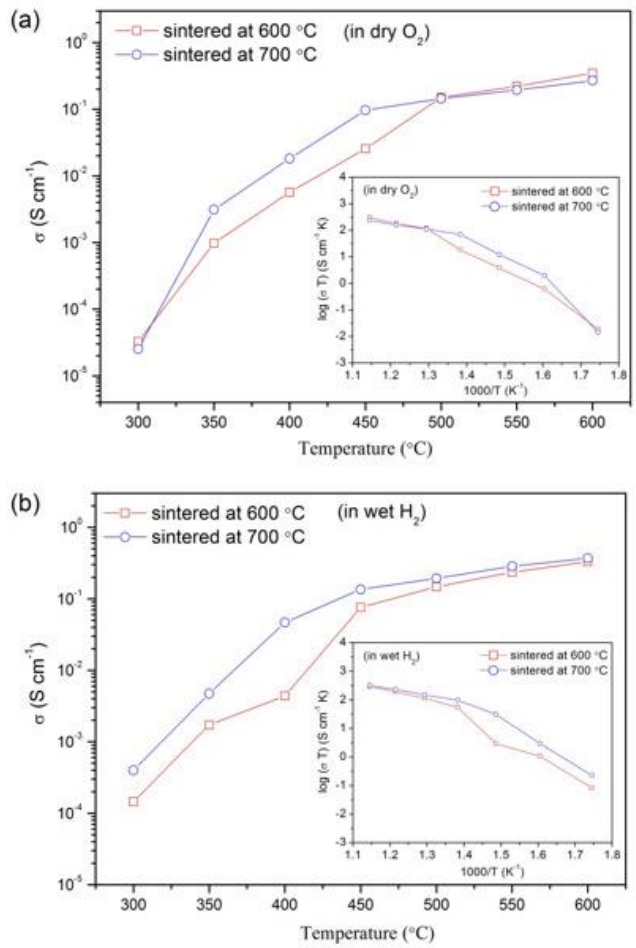

Fig. 7 AC conductivity plot of CDC-carbonate composite against temperature: (a) in dry O_2; (b) in wet 5% H_2-Ar.

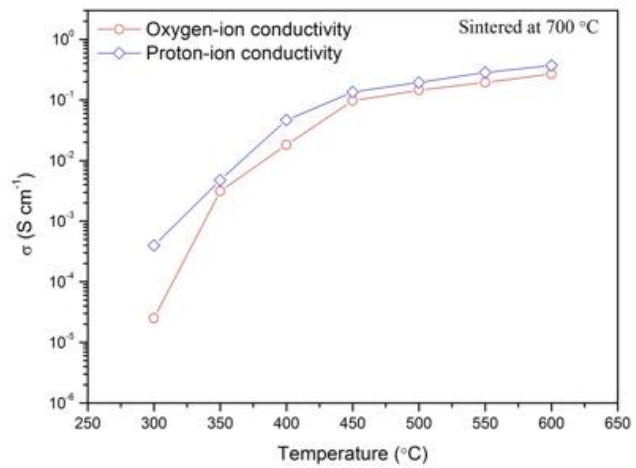

Fig. 8 Comparison between of the oxygen-ion and proton-ion conductivities for pellet sintered at 700°C.

4. Conclusion

In summary, Ca-doped ceria (CDC) was successfully synthesised via sol-gel process. A nanocomposite electrolyte composed of two phases was prepared by mixing 70 wt% of CDC powder with 30 wt% of $(Li/Na/K)_2CO_3$) eutectic salt. A pure phase of CDC with fluorite-type structure was obtained after the heat treatment of its corresponding ash in the air at 700°C for 2 h. The obtained results revealed the thermally stability of the CDC-carbonate composite in the tested atmospheres (oxidising and reducing environments). The electrical properties of CDC-carbonate composite electrolyte were investigated for the sample sintered at two different temperatures (600 and 700°C). The sample sintering temperature played an important role in the electrical properties of the CDC-carbonate nanocomposite electrolyte. At 600°C, the oxygen-ion (O^{2-}) conductivity of the sample sintered at 600°C (0.35 S cm^{-1}) was higher than that of sample sintered at 700°C (0.27 S cm^{-1}). By contrast, at 600°C, the proton ion (H^+) conductivity of the composite electrolyte for sample sintered at 600°C (0.33 S cm^{-1}) was lower than that of sample sintered at 700°C (0.37 S cm^{-1}).

References

Ali, A. Rafique, A. Kaleemullah, M. Abbas, G., Ajmal Khan, M., Ahmad, M.A., Raza, R. (2018) 'Effect of Alkali Carbonates (Single, Binary, and Ternary) on Doped Ceria: A Composite Electrolyte for Low-Temperature Solid Oxide Fuel Cells', *ACS Applied Materials & Interfaces*, 10, pp. 806-818. doi:10.1021/acsami.7b17010.

Amar, I.A. Petit, CTG. Mann, G. Lan, R., Skabara, P.J., Tao, S.W. (2014) 'Electrochemical synthesis of ammonia from N_2 and H_2O based on $(Li,Na,K)_2CO_3$–$Ce_{0.8}Gd_{0.18}Ca_{0.02}O_2$–δ composite electrolyte and $CoFe_2O_4$ cathode', *International Journal of Hydrogen Energy*, 39, pp.4322-4330.

Amar, IA. Petit, CTG. Zhang, L. Lan, R. Skabara, PJ. Tao, SW. (2011) 'Electrochemical synthesis of ammonia based on doped-ceria-carbonate composite electrolyte and perovskite cathode', *Solid State Ionics*, 201, pp. 94-100.

Amar, IA. Sharif, A. Ahwidi, MM. (2017a) 'The ionic conductivity of a nanocomposite electrolyte based on calcium-doped ceria/ternary carbonate', *Journal of Pure & Applied Sciences*, 16, pp. 31-37.

Amar, IA. Sharif, A. Ahwidi, MM. (2018) 'Enhanced ionic conductivity in a composite electrolyte based on cerium oxide-ternary carbonate'. *Journal of Pure & Applied Sciences*, 17, pp. 161-169.

Amar, IA. Sharif, A. Ahwidi, MM. Saleh, F.A. (2017b) 'Electrical properties of gadolinium-doped ceria/ternary carbonate nanocomposite electrolyte', *Paper presented at The 2nd Libyan Conference on Chemistry and its Applications LCCA-2*, Benghazi-Libya, 9-11 May 2017.

Banerjee, S. Devi, PS. Topwal, D. Mandal, S., Menon, K. (2007) 'Enhanced Ionic Conductivity in $Ce_{0.8}Sm_{0.2}O_{1.9}$: Unique Effect of Calcium Co-doping', *Advanced Functional Materials*, 17, pp. 2847-2854.

Cho, PS. Lee, SB. Cho, YH. Kim, D.Y., Park, H.M., Lee, J.H. (2008) 'Effect of CaO concentration on enhancement of grain-boundary conduction in gadolinia-doped ceria', *Journal of Power Sources*, 183, pp. 518-523. doi:https://doi.org/10.1016/j.jpowsour.2008.05.041.

Chourashiya, M. Patil, J. Pawar, S. Jadhav, L. (2008) 'Studies on structural, morphological and electrical properties of $Ce_{1-x}Gd_xO_{2-(x/2)}$', *Materials Chemistry and Physics*, 109, pp. 39-44.

Di, J. Chen, M. Wang, C. Zheng, J., Fan, L., Zhu, B. (2010) 'Samarium doped ceria-$(Li/Na)_2CO_3$ composite electrolyte and its electrochemical properties in low temperature solid oxide fuel cell', *Journal of Power Sources*, 195, pp. 4695-4699.

Fan, L. He, C. Zhu, B. (2017) 'Role of carbonate phase in ceria–carbonate composite for low temperature solid oxide fuel cells: A review', *International Journal of Energy Research*, 41, pp. 465-481.

Fan, L. Wang, C. Chen, M., Zhu, B. (2013) 'Recent development of ceria-based (nano) composite materials for low temperature ceramic fuel cells and electrolyte-free fuel cells', *Journal of Power Sources*, 234, pp. 154-174.

Fu, YP. Chen, SH. Huang, JJ. (2010) 'Preparation and characterization of $Ce_{0.8}M_{0.2}O_{2-\delta}$ (M = Y, Gd, Sm, Nd, La) solid electrolyte materials for solid oxide fuel cells', *International Journal of Hydrogen Energy*, 35, pp. 745-752.

Gao, Z. Mao, Z. Wang, C. Huang, J., Liu, Z. (2009) 'Composite electrolyte based on nanostructured $Ce_{0.8}Sm_{0.2}O_{1.9}$ (SDC) for

low-temperature solid oxide fuel cells', *International Journal of Energy Research,* 33, pp. 1138-1144.

Guan, X. Zhou, H. Liu, Z. Wang, Y., Zhang, J. (2008) 'High performance Gd^{3+} and Y^{3+} co-doped ceria-based electrolytes for intermediate temperature solid oxide fuel cells', *Materials Research Bulletin*, 43, pp. 1046-1054. doi:https://doi.org/10.1016/j.materresbull.2007.04.027.

Inaba, H. and Tagawa, H. (1996) 'Ceria-based solid electrolytes', *Solid State Ionics*, 83, pp. 1-16. doi:https://doi.org/10.1016/0167-2738(95)00229-4.

Jaiswal, N. Upadhyay, S. Kumar, D. Parkash, O. (2015) 'Ionic conduction in Mg^{2+} and Sr^{2+} co-doped ceria/carbonates nanocomposite electrolytes', *International Journal of Hydrogen Energy*, 40, pp. 3313-3320. doi:http://dx.doi.org/10.1016/j.ijhydene.2015.01.002.

Janz, GJ. and Lorenz, MR. (1961) 'Solid-liquid phase equilibria for mixtures of lithium, sodium, and potassium carbonates', *Journal of Chemical and Engineering Data*, 6, pp. 321-323.

Khan, I. Asghar, MI. Lund, PD. Basu, S. (2017) 'High conductive $(LiNaK)_2CO_3Ce_{0.85}Sm_{0.15}O_2$ electrolyte compositions for IT-SOFC applications', *International Journal of Hydrogen Energy*, 42, pp. 20904-20909. doi:https://doi.org/10.1016/j.ijhydene.2017.05.152.

Khan, MA. Raza, R. Lima, RB. Chaudhry, M.A., Ahmed, E. Abbas, G. (2013) 'Comparative study of the nano-composite electrolytes based on samaria-doped ceria for low temperature solid oxide fuel cells (LT-SOFCs)',. *International Journal of Hydrogen Energy*, 38, pp. 16524-16531. doi:https://doi.org/10.1016/j.ijhydene.2013.05.060.

Kim, DJ. (1989) 'Lattice Parameters, Ionic Conductivities, and Solubility Limits in Fluorite-Structure MO_2 Oxide [M= Hf^{4+}, Zr^{4+}, Ce^{4+}, Th^{4+}, U^{4+}] Solid Solutions', *Journal of the American Ceramic Society*, 72, pp. 1415-1421.

Li, S. Wang, X. Zhu, B. (2007) 'Novel ceramic fuel cell using non-ceria-based composites as electrolyte', *Electrochemistry Communications*, 9, pp. 2863-2866. doi:http://dx.doi.org/10.1016/j.elecom.2007.10.010.

Li, Y. Rui, Z. Xia, C. Anderson, M., Lin, Y.S. (2009) 'Performance of ionic-conducting ceramic/carbonate composite material as solid oxide fuel cell electrolyte and CO_2 permeation membrane', *Catalysis Today*, 148, pp. 303-309.

Liu, Q. Tian, Y. Xia, C. Thompson, L.T., Liang, B., Li, Y. (2008) 'Modeling and simulation of a single direct carbon fuel cell', *Journal of Power Sources*, 185, pp. 1022-1029.

Liu, W. Liu, Y. Li, B. Sparks, T.D., Wei, X., Pan, W. (2010) 'Ceria (Sm^{3+}, Nd^{3+})/carbonates composite electrolytes with high electrical conductivity at low temperature', *Composites Science and Technology*, 70, pp. 181-185.

Ma, Y. Wang, X. Khalifa, HA. Zhu, B., Muhammed, M. (2012) 'Enhanced ionic conductivity in calcium doped ceria e Carbonate electrolyte: A composite effect', *International Journal of Hydrogen Energy*, 37, pp. 19401-19406.

Mogensen, M. Sammes, NM. Tompsett, GA. (2000) 'Physical, chemical and electrochemical properties of pure and doped ceria', *Solid State Ionics*, 129, pp. 63-94. doi:https://doi.org/10.1016/S0167-2738(99)00318-5.

Muhammed, Ali SA. Rosli, RE. Muchtar, A. Sulong, A.B., Somalu, M.R., Majlan, E.H. (2015) 'Effect of sintering temperature on surface morphology and electrical properties of samarium-doped ceria carbonate for solid oxide fuel cells', *Ceramics International*, 41, pp. 1323-1332. doi:https://doi.org/10.1016/j.ceramint.2014.09.064.

Patra, H. Rout, SK. Pratihar, SK. Bhattacharya, S. (2011) 'Effect of process parameters on combined EDTA–citrate synthesis of $Ba_{0.5}Sr_{0.5}Co_{0.8}Fe_{0.2}O_{3-\delta}$ perovskite', *Powder Technology*, 209, pp. 98-104 doi:https://doi.org/10.1016/j.powtec.2011.02.015.

Raza, R. Qin, H. Fan, L. Taked, K., Mizuhat, M., Zhu, B. (2012) 'Electrochemical study on co-doped ceria–carbonate composite electrolyte', *Journal of Power Sources*, 201, pp. 121-127.

Raza, R. Wang, X. Ma, Y. Zhu, B. (2010) 'Study on calcium and samarium co-doped ceria based nanocomposite electrolytes', *Journal of Power Sources*, 195, pp. 6491-6495.

Ristoiu, T. Petrisor-Jr, T. Gabor, M. Rada, S., Popa, F., Ciontea, L., Petrisor, T. (2012) 'Electrical properties of ceria/carbonate nanocomposites', *Journal of Alloys and Compounds*, 532, pp. 109-113.

Shannon, RT. and Prewitt, CT. (1969) 'Effective ionic radii in oxides and fluorides', *Acta Crystallographica Section B: Structural Crystallography and Crystal Chemistry*, 25, pp. 925-946.

Singh, K. Acharya, S. Bhoga, S. (2007) 'Low temperature processing of dense samarium-doped CeO_2 ceramics: sintering and intermediate temperature ionic conductivity', *Ionics*, 13, pp. 429-434

Steele, BCH. (2000) 'Appraisal of $Ce_{1-y}GdyO_{2-y/2}$ electrolytes for IT-SOFC operation at 500 °C', *Solid State Ionics*, 129, pp. 95-110. doi:https://doi.org/10.1016/S0167-2738(99)00319-7.

Tanwar, K. Jaiswal, N. Sharma, P. Kumar, D., Parkash, O. (2018) 'Structural analysis of $Ce_{0.83}Dy_{0.14}Ca_{0.03}O_{1.90}$ (CDC) and enhanced electrical conductivity of its composites with alkali carbonates for LT-SOFCs', *Journal of Alloys and Compounds*, 741, pp. 532-541. doi:https://doi.org/10.1016/j.jallcom.2018.01.128.

Wang, F-Y. Chen, S. Cheng, S. (2004) 'Gd^{3+} and Sm^{3+} co-doped ceria based electrolytes for intermediate temperature solid oxide fuel cells', *Electrochemistry Communications*, 6, pp. 743-746. doi:https://doi.org/10.1016/j.elecom.2004.05.017.

Wang, X. Ma, Y. Li, S. Kashyout, A.H., Zhu, B., Muhammed, M. (2011) 'Ceria-based nanocomposite with simultaneous proton and oxygen ion conductivity for low-temperature solid oxide fuel cells', *Journal of Power Sources*, 196, pp. 2754-2758. doi:https://doi.org/10.1016/j.jpowsour.2010.11.033.

Wang, X. Ma, Y. Zhu, B. (2012) 'State of the art ceria-carbonate composites (3C) electrolyte for advanced low temperature ceramic fuel cells (LTCFCs)', *International Journal of Hydrogen Energy*, 37, pp. 19417-19425.

Xia, C. Li, Y. Tian, Y. Liu, Q., Zhao, Y., Jia, L., Li, Y. (2009) 'A high performance composite ionic conducting electrolyte for intermediate temperature fuel cell and evidence for ternary ionic conduction', *Journal of Power Sources*, 188, pp. 156-162.

Xia, Y. Bai, Y. Wu, X. et al. (2011) 'The competitive ionic conductivities in functional composite electrolytes based on the series of M-NLCO (M = $Ce_{0.8}Sm_{0.2}O_{2-\delta}$, $Ce_{0.8}Gd_{0.2}O_{2-\delta}$, $Ce_{0.8}Y_{0.2}O_{2-\delta}$; NLCO = $0.53Li_2CO_3$–$0.47Na_2CO_3$)', *International Journal of Hydrogen Energy*, 36, pp. 6840-6850.

Zarkov, A. Stanulis, A. Salkus, T. Kezionis, A. Jasulaitiene, V. Ramanauskas, R. Tautkus, S. Kareiva,A. (2016) 'Synthesis of nanocrystalline gadolinium doped ceria via sol–gel combustion and sol–gel synthesis routes', *Ceramics International*, 42, pp. 3972-3988. doi:https://doi.org/10.1016/j.ceramint.2015.11.066.

Zhu, B. Albinsson, I. Andersson, C. Borsand, K. Nilsson, M. Mellander, BE. (2006) 'Electrolysis studies based on ceria-based composites', *Electrochemistry Communications*, 8, pp. 495-498. doi:http://dx.doi.org/10.1016/j.elecom.2006.01.011.

Zhu, B. Fan, L. Lund, P. (2013) 'Breakthrough fuel cell technology using ceria-based multi-functional nanocomposites', *Applied energy*, 106, pp. 163-175.